Spatial Statistical Model for the Spread of Dwarf Mistletoe Within and Between Stands

Donald C.E. Robinson
Brian W. Geils
John A. Muir

Abstract—Dwarf mistletoes affect the growth and survival of many conifer species in North America. Interactions between the host and pathogen influence spread, intensification, and stand development. These interactions are especially complex in stands with several tree species, multiple storys, and irregular patterns of tree distribution. For such stands, we developed a model of mistletoe dynamics linked to FVS. The model simulates the development and dispersal of mistletoe seeds and describes infection distribution by dwarf mistletoe rating (DMR). The stand-level model includes several important features such as the spatial arrangement of trees, the spatial autocorrelation of trees with similar amounts of mistletoe infection, the dynamics of seed flight, the effect of crowns intercepting and inhibiting infection spread, and the light environment that strongly affects the life history of dwarf mistletoes. Model input requirements are modest: at a minimum, only an FVS tree list that includes DMR is required. Users may either enter parameters for the patterns of tree distribution and mistletoe patchiness or accept default values. User-determined values can be computed from many standard survey designs or set from experience with similar situations. Default values represent many typical stands. Simulations based on data from uneven-aged ponderosa pine and coastal western hemlock stands show reasonable projections of stand-level changes in mistletoe incidence and severity over several decades, and plausible responses to silvicultural management scenarios. Recent work is also described that provides a theoretical basis for simulating spread between stands. This between-stand model is currently being implemented using the Parallel Processing Extension to FVS.

Dwarf mistletoes (*Arceuthobium*) are among the most widespread and serious conifer pathogens in western North American forests. Up to half of lodgepole pine and Douglas-fir forests and over one-third of ponderosa pine forests in the Central and Southern Rockies are affected by dwarf mistletoe (Hawksworth and Scharpf 1984). Infection by mistletoe reduces growth, survival, and reproductive potential of many commercially important tree species, resulting in estimated losses of more than 11 million m^3 per year of merchantable timber in the United States (Drummond 1982). Development of silvicultural prescriptions to control the tree-to-tree spread of mistletoes within stands has been the subject of extensive research efforts for many years (Van Sickle and Wegwitz 1978; Hawksworth and others 1987; Hawksworth and Johnson 1989). The goal of these prescriptions has been to limit the intensification of already established infections and to reduce the potential to spread to uninfested trees. Spread across stand discontinuities is also recognized as an important factor when designing spatial cutblock patterns in variable retention silviculture.

While control of mistletoe can sometimes be achieved silviculturally, planning cost-effective treatments must be done within the larger context of landscape- and stand-level management planning. Increased use of forest growth and yield models to assist forest managers in planning silvicultural operations and their expected consequences on economic returns have created a need for accurate prediction of the dynamics of dwarf mistletoe response to stand-level management, and the ability to accommodate nonclearcutting practices. Our objectives were to: (1) develop a model of the mistletoe infection dynamics that can be used to assess stand-level silvicultural activities for mistletoe management; and (2) extend the conceptual model to accommodate the simulation of spread across stand discontinuities.

Dwarf Mistletoe Spread and Intensification

Two aspects of the life history of dwarf mistletoe are critical for predicting mistletoe spread and intensification: first, the mechanics of seed dispersal, and second, the establishment, incubation, and reproduction of mistletoe plants on their hosts. Generally, there is a unique relationship between the host tree species and its associated dwarf mistletoe species, and seeds will not successfully infect a tree of another species. Dwarf mistletoes are dioecious plants that reproduce only from seeds borne on shoots. Seed dispersal begins when a mature fruit explosively discharges its seed in ballistic flight. Unlike other mistletoes, which are primarily dispersed by birds, the dwarf mistletoes rely almost exclusively on ballistic spread. Birds and mammals are important for the rare, long-distance dissemination of seeds to new infection centers.

The physical process of dispersal brings the mistletoe seed to the location where it establishes a new infection. The incubation period of newly established plants varies greatly but is typically 3 to 4 years (Hawksworth and Wiens 1996).

In: Crookston, Nicholas L.; Havis, Robert N., comps. 2002. Second Forest Vegetation Simulator Conference; 2002 February 12–14; Fort Collins, CO. Proc. RMRS-P-25. Ogden, UT: U.S. Department of Agriculture, Forest Service, Rocky Mountain Research Station.

Donald C.E. Robinson is a Systems Ecologist, ESSA Technologies Ltd., Third Floor, 1765 West 8th Avenue, Vancouver, B.C., Canada. V6J 5C6. drobinson@essa.com. Brian W. Geils is a Research Plant Pathologist, USDA Forest Service, Rocky Mountain Research Station, Southwest Forest Science Complex, 2500 South Pine Knoll Drive, Flagstaff, AZ, U.S.A. 86001-6381. bgeils@fs.fed.us. John A. Muir is a Forest Pathologist, Silviculture Practices Section, B.C. Ministry of Forests, PO Box 9513, Stn. Prov. Govt, Victoria, B.C., Canada. V8W 9C2. john.muir@gems1.gov.bc.ca

Generally, 1 to 2 years then elapse from shoot appearance to initial flowering. Individual plants may persist for many decades. Because they rely upon the host for nutrition and because reproductive success does not require annual seed production, mistletoes can persist without aerial shoots, as latent infections. Little is known of the physiological mechanisms regulating shoot production, but it appears that shoot production and flowering are suppressed in the low light and nutrition environment of shaded lower crowns (Shaw and Weiss 2000). Opening the canopy by removing surrounding trees, as is often done to thin or regenerate a stand, commonly results in a proliferation of mistletoe shoots on the residual trees.

Ballistic dispersal and parasitism are critical to mistletoe population dynamics. Ballistic dispersal is effective for short-range dissemination only, and parasitism requires a living host. Consequently, mistletoe plants are found clustered within trees, and infected trees are clustered into infested groups. The spatial pattern of mistletoe populations therefore operates across a range of scales: the tree, neighborhood, and stand. The average level of infection is usually described by an index of the amount of host crown affected: the dwarf mistletoe rating (DMR) system (Hawksworth 1977). Each crown third is rated 0 if it is apparently not infected, 1 if less than half is infected, or 2 if more than half is infected. The DMR system allows infection to be quantified in various ways: by crown thirds, for the whole tree, or by averaging across a collection of trees, for a group or stand of trees.

We define *spread* as the establishment of mistletoe infection in previously uninfected trees, and *intensification* as the establishment of new mistletoe infections within infected trees. Spread and intensification are influenced by the same factors and are complementary aspects of the same process. Dispersal is primarily affected by the physical configuration of the tree: crown density and distribution; and by stand species composition. Establishment, incubation, and reproduction are determined by weather, genetic, and other biological factors.

The Model

A number of dwarf mistletoe models have been developed to assist forest managers in planning silvicultural operations and estimating effects on yield. These models range from projecting whole-stand impacts (for example, Myers and others 1971, Edminster and others 1991) to the explicit simulation of the effects of the spatial arrangement of trees (for example, Strand and Roth 1976, Bloomberg and Smith 1982).

The model described in this paper simulates dwarf mistletoe spread and intensification at an intermediate spatial resolution in which the transmission of dwarf mistletoe is the outcome of spatial relationships between infected and uninfected trees. In the model, height and canopy relationships are *explicit* and stem location relationships are *statistical*, based on the spatial distribution of trees at the 14-m scale of ballistic spread. Those parts of the model that are explicitly spatial operate at a 2-m resolution. The model operates on an annual time step and is able to simulate infection dynamics in patchy multispecies, multistoried stands. It does not simulate long-distance transmission of mistletoe and is restricted to spread from ballistic seed flight. It is linked to the Dwarf Mistletoe Impact Modelling system (DMIM; Hawksworth and others 1995), an extension to the FVS model (Stage 1973; Wykoff and others 1982). Dwarf mistletoe impacts, reduced diameter increment, and reduced survival for severely infected trees, are modelled using the DMIM system.

Model users are provided with the means to parameterize the model. The detailed model structure and user-control are fully documented in Robinson and others (1994) and in Hawksworth and others (1995). Modelling behavior studies are described in Robinson and others (2000) and in Robinson and Geils (in preparation). The main features of the model are summarized below.

Life History

In the simplest case, new infections progress from an immature through an incubation stage and finally produce an active (flowering) adult that contributes to the DMR classification. The passage from immature to incubation status is modeled with a default delay of 4 years. Passage to the reproductive stage depends on the amount of light available in the crown third. If light decreases to the point that an active infection cannot be sustained, the infection regresses to a nonflowering suppressed state. These life-history dynamics and stages are summarized in figure 1. Light plays an important role in most of the transitions between life history stages and takes the form of a height-dependent extinction curve. As described below, this curve is dynamically generated using a simulated stem map and a model of the canopy.

Light and Opacity

The presence or absence of light is critical to the maturation of incubating infections and to the activation or suppression of mature flowering plants. The model uses the concept of stand-average opacity to simulate the reduction of light by foliage, branches, and stems. In doing so, it is able to estimate the proportion of incident light at different heights above the ground, and by the same mechanism account for the interception of seeds in ballistic flight. Stands may be made up of trees of different species, height, crown shape, length, and foliage opacity. To account for this complexity, stand-average opacity is computed by Monte Carlo simulation. At the beginning of each time step, a 1-ha stand simulation is made. Each tree is represented in proportion to its density in the stand. Beginning at the ground and extending upward in 2-m steps, the structure of each layer is simulated with simplified circular discs of canopy, each representing the crown diameter of trees at that height. Canopy geometry is computed by the COVER model (Moeur 1985) (fig. 2). After simulating all the stem locations, the stand-average opacity at each height is a function of the amount of space unoccupied by canopy, combined with the canopy opacity of the space occupied by foliage. Stand-average opacity is then used to reduce the amount of light

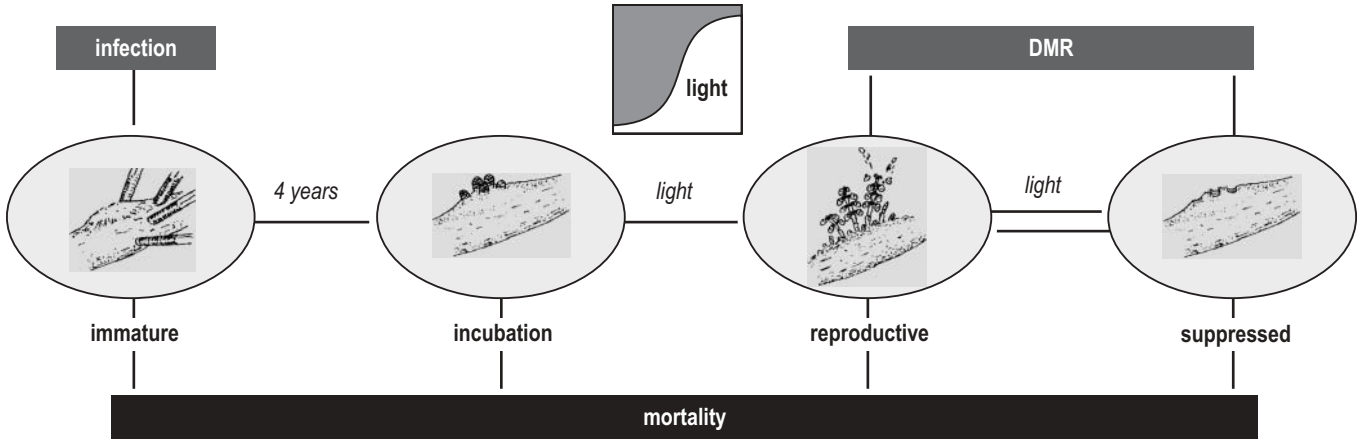

Figure 1—The model simplifies dwarf mistletoe life history into four stages. Light drives the progress of incubating infections to reproductively active individuals, and to and from the suppressed pool.

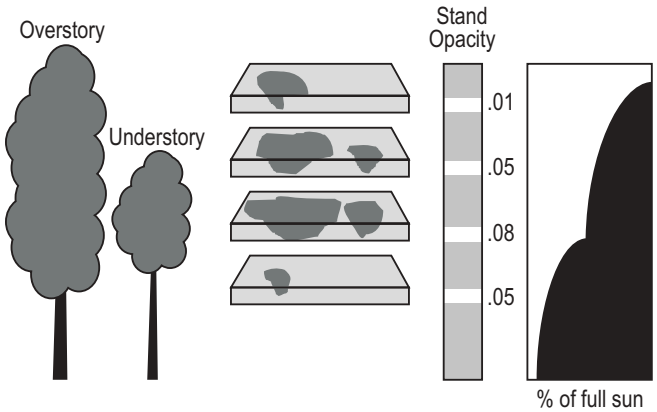

Figure 2—An estimate of stand-average opacity is made by simulating the crown diameter at each height in the stand. Light penetrating the stand from above is blocked by crowns, and less light is available at lower heights (right panel). The ability of crowns to block light varies with stem density and by species. For example, pines allow more light to pass than western hemlock.

transmitted from the top of the stand to the ground. Because light extinction is cumulative, a decay curve results.

Stem Clumpiness

Seeds spread ballistically from a source tree to a target tree. For an infection to be transmitted successfully, two trees must have compatible heights and be in the same neighborhood. The local neighborhood of each target tree can be regular, random, or clumped. As the left part of figure 3 shows, the model simulates stem spacing by placing a target tree at the center of a bulls-eye, surrounded by 2 m rings. Source trees are then selected and simulated as if they were located in each of the concentric rings. Placing a target at the center of a bulls-eye with source trees at discrete distances allows the infection field of each source tree to overlap the canopy of the target, simulating the dynamics of spread.

For each of the concentric rings, the expected number of stems is the average stem density of the whole stand multiplied by the area in the ring. A ring is defined by its inner and outer radius, r_i and r_o. The distribution for an inner disc with radius r_i (the r_i disc) is derived first, giving the probability of sampling $x=0,1,2,3...$ trees in the inner disc. The same method is followed for the larger r_o disc, as shown in figure 3. The expected distribution of trees in the ring is then defined by the distribution of trees found in disc r_o that are not already in disc r_i. The distribution is generated by counting all the combinations of tree numbers on the two discs that would give rise to an observation of a particular number of trees in the ring (equation 1). In equation 1, the probability generating function, P, can be binomial, poisson, or negative binomial. The upper tail of the distribution drops

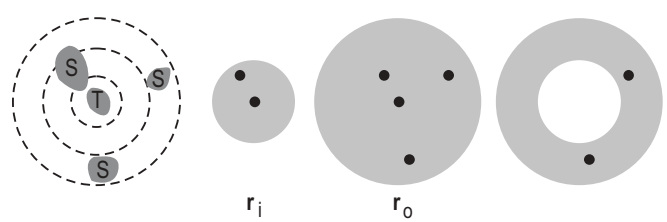

Figure 3—At left, source trees, S, surrounding each target tree, T, are selected based on an underlying spatial clumping function (for example, binomial). Samples in each ring are based on the conditional distribution functions produced by overlapping inside and outside discs, r_i and r_o. The example shows one possible way in which a ring with two source trees could be simulated from samples from inside and outside discs. Actual positions around the disc are not necessary for the simulation.

off rapidly, and in practice the summation over j and k usually converges with fewer than 20 terms.

$$P(x = n \mid r_i, r_o) = \frac{\sum_{j=o}^{\infty} P(x = j \mid r_o)\, P(x = j - n \mid r_i)}{\sum_{k=o}^{\infty} \sum_{j=k}^{\infty} P(x = j \mid r_o)\, P(x = j - k \mid r_i)}; n > 0 \qquad [1]$$

The denominator term scales the probability distribution. This scaling is necessary because the two disc samples are not independent. The r_i disc lies completely inside the r_o disc, and therefore some tree counts are impossible. For example, if a sample of size 3 is observed in the inner disc r_i, a sample of 2 or fewer can never be observed in the outer disc r_o. The double summation in the denominator adjusts the distribution so that the probabilities over all sample sizes sum to one.

Infection Patchiness

In addition to creating a local neighborhood around each target tree, the model simulates positive autocorrelation among infection classes, resulting in patches of infection. The autocorrelation results in an increased likelihood that trees of similar DMR are neighbors compared to trees of unlike DMR. The stem-mapped Log Cabin plot shown in Dixon and Hawksworth (1979) and the Wind River site (Shaw and others 2000) both give good examples of such patches. Although the existence of patches is well documented, modelling their explicit arrangement is not reasonable for a nonspatial growth model. We have therefore modelled the autocorrelation structure of DMR with a simple function (equation 2), an exponential decay curve driven by the magnitude of DMR difference between a target and its potential neighbors. Equation 2 gives a modified density estimate, ρ'_i, for each DMR class, i, surrounding a target tree of DMR t.

$$\rho'_i = \rho_i e^{\alpha |t-i|} \frac{\sum_{j=0}^{6} \rho_j}{\sum_{j=0}^{6} \rho_j e^{\alpha |t-j|}} \qquad [2]$$

This difference-driven weighting assigns greater density to neighboring source trees with DMR similar to the DMR of the target tree, and less density to trees with unlike DMR. It allows the local DMR to vary in different target tree neighborhoods, while maintaining the observed stand-average DMR. To preserve stand-level statistics, reducing the likelihood of finding a source tree having a different DMR class implies a corresponding increase in the density of similar-DMR sources in other neighborhoods. Equation 2 preserves this symmetric property of target-source differences in DMR: trees "taken away" from one neighborhood are "put back" in another neighborhood, so that the stand density of each DMR class is preserved. These properties are illustrated in table 1 (setting $\alpha = -0.5$).

The term can be estimated from stem-mapped data by comparing the density of each source DMR class observed around each target DMR tree. Predictions made by equation 2 are compared against observed stem map densities, generating a range of χ^2 over a range of values for α. Minimizing χ^2 then gives the best choice of α. Results from an analysis of six sites (four from a long-term study in the Grand Canyon National Park; one from Fort Valley, and one from the Wind River site; J.J. Smith, personal communication) are shown in table 2. Three of the sites have repeated measures but show no consistent change in α over time. The mean of all 28 observations is $\alpha = -0.103$ (SD = 0.075).

Ballistic Seed Dispersal

Because of physical constraints on seed flight, infection is usually transmitted laterally and downward from an infection source. An infection in a higher tree will usually expose a lower neighbor to infection, but not the reverse. The model uses encoded and simplified ballistic seed trajectories based on the following characteristics: 24 m s^{-1} initial velocity (Hinds and Hawksworth 1965); 7.5 m s^{-1} terminal velocity (Hawksworth 1959); uniform random angle of discharge; and aerodynamic drag represented as a quadratic function of velocity. These assumptions produce the dispersal pattern shown in figure 4. The 14-m lateral limit is consistent with field observations (for example, Hawksworth 1961).

Table 1—An example of spatial autocorrelation setting $\alpha = -0.5$ The left side of the table shows the stand-average density of each DMR class. Rows of the right table show the neighborhood density of source trees around each target DMR class (columns). In each case, the overall stand density is preserved. Weighted sums by neighborhood density (right-most column) show that the stand-average DMR densities are also preserved.

DMR	Stand avg. density	Source DMR	Target DMR class 0	1	2	3	4	5	6	Wtd. density
0	45	0	80	47	29	21	17	15	13	45
1	25	1	27	43	26	20	16	14	12	25
2	32	2	21	33	56	41	33	29	25	32
3	17	3	7	11	18	36	29	26	22	17
4	12	4	3	5	8	16	34	30	26	12
5	3	5	0	1	1	2	5	12	11	3
6	5	6	0	1	1	2	5	12	29	5
Total	139	Total	139	139	139	139	139	139	139	

Table 2—Observed values of α, the autocorrelation parameter, at six sites.

	Stand					
Year	GC11	GC12	GC22	GC06	Ft. Valley	Wind R
1950		–0.13	–0.07			
1952				0.06		
1955		–0.12	–0.06	0.00		
1961		–0.15	–0.08	–0.01		
1966		–0.14	–0.07	–0.03		
1970		–0.15	–0.03	–0.04		
1979		–0.16				
1982		–0.20	–0.07	–0.10		
1986		–0.25				
1988				–0.13		
1990		–0.27	–0.02	–0.14		
1997	–0.07	–0.18			–0.12	–0.15

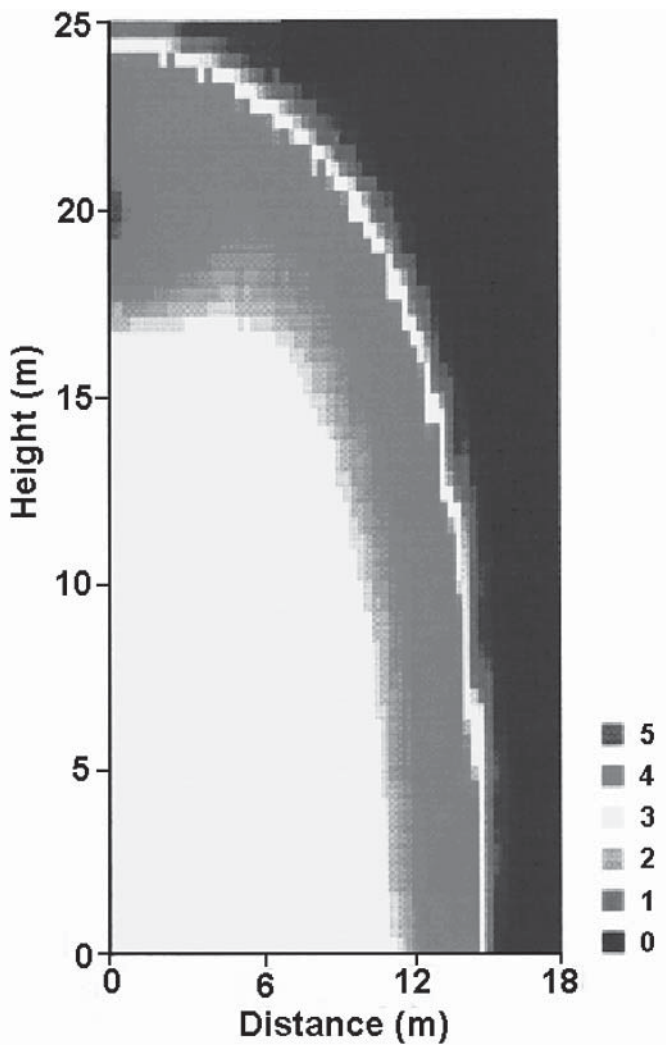

Figure 4—The aerodynamic simulation of ballistic flight produces a field of trajectories. The maximum lateral discharge is about 14 m, and the maximum rise above the point of discharge (20 m in the figure) is about 6 m. Discharge is heaviest near the outer margin of the discharge envelope. The scale is log-transformed relative seed density.

Examples of Model Behavior

Grand Canyon —Ponderosa Pine

In 1950, Frank Hawksworth initiated a study of dwarf mistletoe control in several fixed area plots of moisture-limited ponderosa pine on the south rim of the Grand Canyon. We used data from plot GC12, an untreated 4-ha fixed area plot that was stem-mapped and monitored for its tree and mistletoe characteristics (tree condition, dbh, height, DMR). Stand examinations were made in 1950, 1955, 1961, 1966, 1970, 1979, 1982, 1986, 1990, and 1997. The oldest trees are currently about 250 years. Ingrowth had been minimal for most of the period. Stand basal area of original trees declined from 11.5 m^2 ha^{-1} in 1950 to 5.3 m^2 ha^{-1} in 1990. (The most recent 1997 inventory was not included in this analysis and includes the recent ingrowth.)

We carried out numerous model simulations with these data to examine the model's sensitivity to opacity, clumping, and patchiness, comparing those runs to the empirical observations. The results in figure 5 show the influence of α, which controls the patchiness of infections. When $\alpha = -2.50$, infection patches are tightly focused, resulting in high mortality, limited spread to uninfected trees, and declining stand DMR. Conversely, with $\alpha = 0.0$ the infections are evenly spread throughout the stand, resulting in extensive spread. When $\alpha = -0.30$ the predicted stand DMR follows the inventory estimates quite closely. The mean estimate over the 50-year period is $\alpha = -0.18$ (see table 2).

Vancouver Island—Western Hemlock

Through the courtesy of Weyerhaeuser Canada Ltd., we were provided with a number of 1-ha inventories from Vancouver Island, B.C. The stands are predominantly western hemlock and range from dwarf mistletoe-free to moderately infested. To study response to management, we selected a young, lightly infected stand (age = 53 years in 1987; SI = 24 m; QMD = 15 cm; BA = 44 m^2 ha^{-1}; stand DMR = 1.2). The stand was initially understocked. An initial planting was therefore simulated, to give a target stocking level of 1,200 stems ha^{-1}.

The simulations follow a block design, with two retention scenarios and three regeneration scenarios. Shelterwood harvests left 15 and 25 percent of the basal area following an entry at age 100. Three regeneration scenarios were simulated: (1) no manual planting following entry; (2) planted using the original species mixture following entry; and (3) planted using an 80:20 hemlock:cedar mix following entry. In all three scenarios a small amount of simulated natural regeneration was added in each cycle. At the time of stand entry, 15 percent mortality was applied to the advanced regeneration, and natural regeneration was cancelled in the planted stands for 20 years. Finally, the residual overstory was removed 20 years after the stand entry, allowing the regenerating stand to continue growing. Some results of these simulations are shown in figure 6. The figure shows two measures of infection: stand DMR in the upper panels and infected trees/ha in the lower panels.

In each of the simulations, the first entry is responsible for a dramatic decline in DMR and in the number of infected

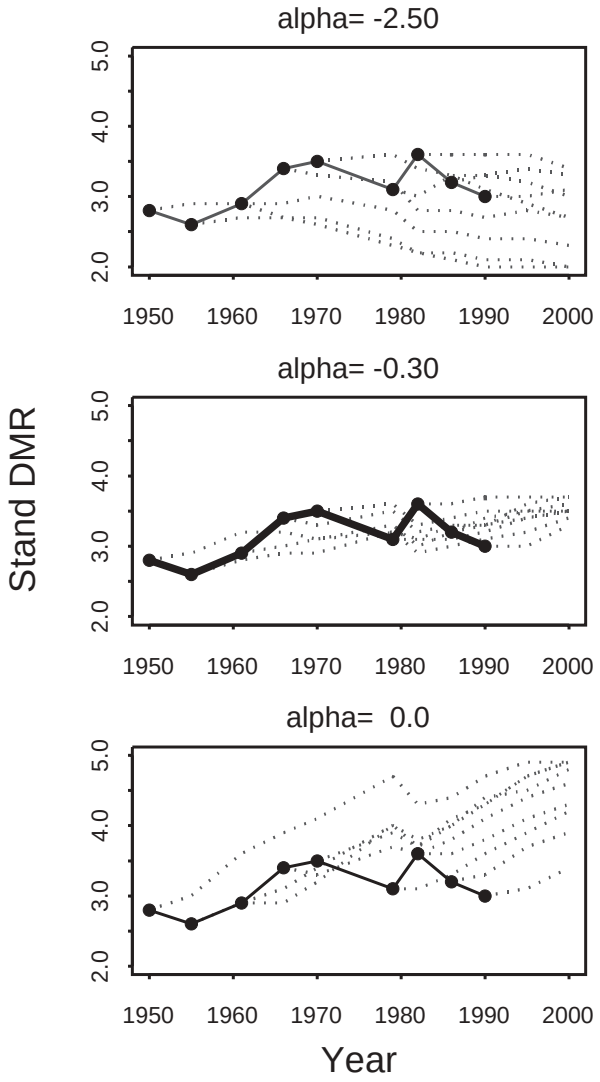

Figure 5—Sensitivity to the choice of the autocorrelation parameter, α (see equation 2) is shown in simulations from the GC12 plot. The heavy line in each pane shows the inventory-based estimate of stand DMR over time. Lighter lines show the model projection of DMR, starting at each inventory date. See text for further interpretation.

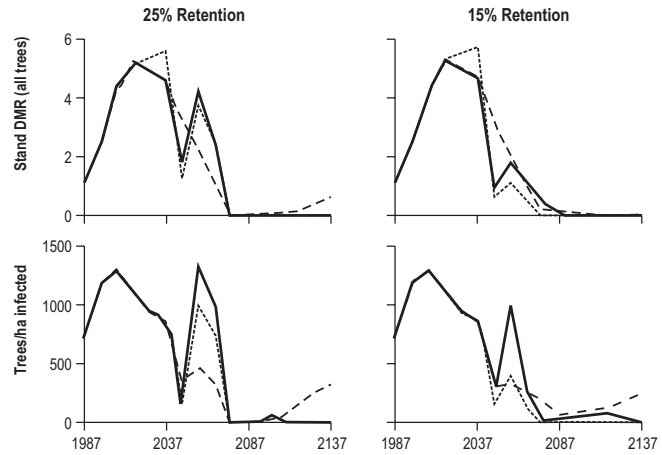

Figure 6—The model's sensitivity to management actions are shown in simulations from the Vancouver Island plot: variable levels of retention, different regeneration scenarios, and different species mixtures. The representation of overstory and understory relationships is responsible in large measure for this sensitivity. See text for further interpretation. Dashed line — unplanted following entry; solid line — planted with original mixture following entry; dotted line — planted with cedar mixture following entry. See text for additional details.

trees. The decline is less precipitous in the unplanted scenario for two reasons. First, the scenario continues to regenerate in the period after the first entry and therefore carries more mistletoe infection in the advanced regenerating trees. Second, the two planting scenarios "dilute" stand DMR with large numbers of initially uninfected seedlings. After thinning, infection levels and DMR both rebound as the infection is transferred from the residual overstory to the new understory trees. As expected, the 25 percent retention scenarios always transmit more mistletoe because they contain almost twice as many overstory trees as the 15 percent scenario. Likewise, regeneration scenarios that incorporate western redcedar all result in lower transmission success. This reduction is achieved through the physical blocking of seeds and because the infection measures are based on summing over both western redcedar (which is never infected) and western hemlock.

The success of the postentry mistletoe flush is transient in most of the simulations and is nearly always quenched by the subsequent second entry removal of the residual overstory. The young regenerating stands appear to "outrun" the new infestation because they are adding sufficient height annually so that they outgrow and then suppress the more slowly advancing mistletoe. In some scenarios — notably the unplanted — the infection is successfully transferred to the next generation because of its greater incidence in the more abundant advanced regeneration.

Spread Across Boundaries

To meet habitat conservation goals, group retention harvesting systems are being considered in some harvest plans (Bill Beese, Weyerhaeuser Canada Ltd., Nanaimo, B.C.; personal communication). In these scenarios, retained patches containing dwarf mistletoe have the potential to spread across patch boundaries and into young regrowing areas. The need to understand and project the future state of these regrowing stands motivated us to adapt the spatial statistical framework to accommodate spread across boundaries. As figure 7 shows, the first step in extending the existing framework is to superimpose a boundary line across the local neighborhood of target trees. Conceptually, the stand structure of the adjacent stand then contributes any dwarf mistletoe influence onto trees in the index stand.

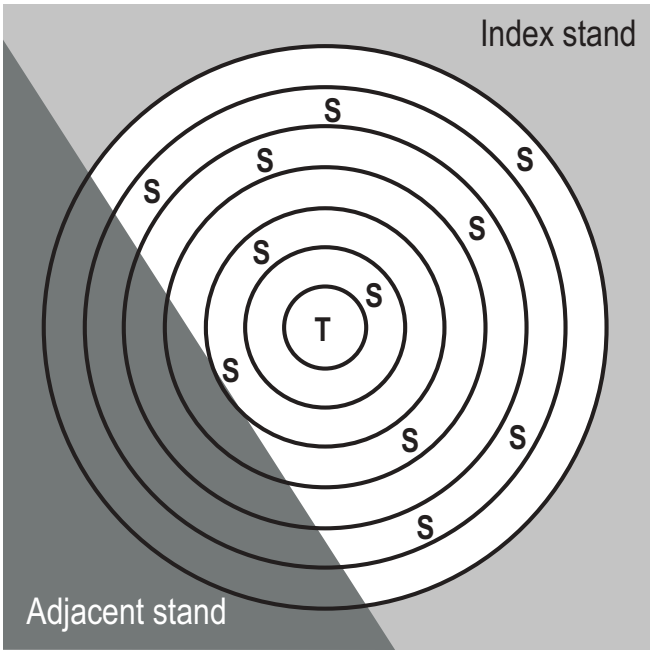

Figure 7—Between-stand spread is simulated using the same framework as the single-stand model, superimposing a boundary across the local neighborhood of the target tree, T. Source trees (S) and stand structure of the adjacent stand then contribute to the spread of DM onto trees in the index stand.

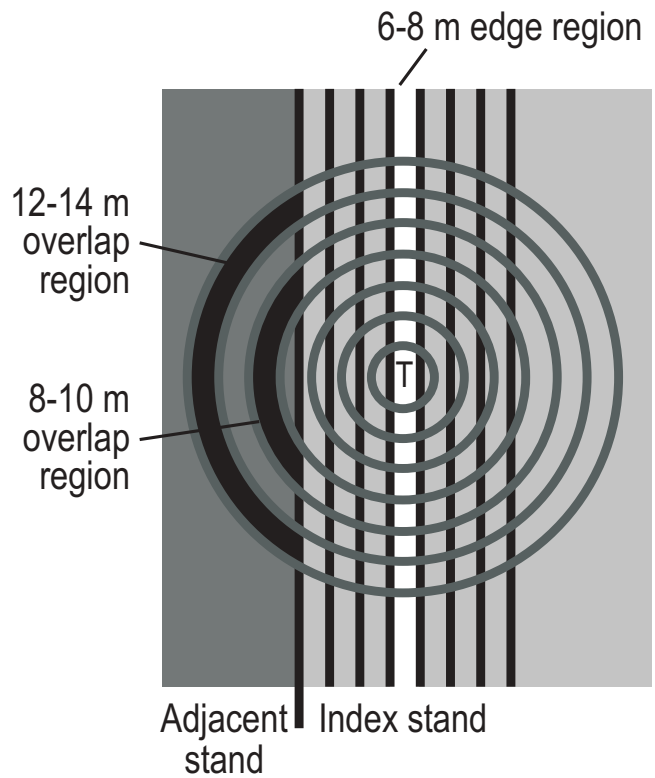

Figure 8—In this example, the likelihood that a target tree, T, lies within 6 to 8 m of the adjacent stand depends upon the proportion of stand area in that edge region. The amount of area found in ring samples in the adjacent stand (for example, the 8 to 10 m overlap region) depends on the amount of overlap of the target tree neighborhood. DM present in source trees found in the adjacent stand can then be included for the target tree.

Figure 8 shows a target tree, T, adjacent to a stand boundary. The likelihood of finding a tree in this location depends on the proportion of the stand area within a given "edge band." If a target lies in a band, the influence of source trees in the adjacent stand then depends on the amount of overlap into the adjacent stand. These relationships are being modelled using the programming infrastructure of the Parallel Processing Extension (PPE: Crookston and Stage 1991), combined with a map preprocessing step using spatial numerical integration to derive the measures of relative and absolute area in edge bands and in adjacent stands.

Conclusions

A spatial statistical model was developed to represent several important features of the life history and distribution of dwarf mistletoe in complex stands—namely, mistletoe latency and mortality, stem clumpiness, and infection patchiness. Several example situations demonstrate that parameter estimation is not an impediment to use and that projections produce reasonable results that are useful for assessing management alternatives within infested stands. The spatial statistical framework has been extended to a slightly larger scale and is able to model the spread of dwarf mistletoe across stand or treatment discontinuities.

Acknowledgments

We express our appreciation to the more than 30 foresters, plant pathologists, and modellers (see Robinson and others 1994 for a complete listing) who have contributed their time and expertise to the development of this model.

Bill Beese and Nick Smith (Weyerhaeuser Canada Ltd., Nanaimo) provided us with suggestions for hemlock management systems and with updated inventory data. Mark Perdue (Department of Forest Sciences, UBC) provided us with guidance during the development and testing of plausible regeneration and stocking scenarios for the Vancouver Island simulations. Glenn Sutherland carried out the Vancouver Island simulations.

We thank Kelly Robson at ESSA Technologies, who prepared the figures.

References

Bloomberg, W. J.; Smith, R. B. 1982. Measurement and simulation of dwarf mistletoe infection on second-growth western hemlock on southern Vancouver Island. Can. J. For. Res. 12: 280-291.

Crookston, N. L.; Stage, A. R. 1991. User's guide to the Parallel Processing Extension of the Prognosis Model. Gen. Tech. Rep. INT-281. Ogden, UT: U.S. Department of Agriculture, Forest Service, Intermountain Research Station. 88 p.

Dixon, G. E.; Hawksworth, F. G. 1979. A spread and intensification model for southwestern dwarf mistletoe in ponderosa pine. For. Sci. 25: 43-52.

Drummond, D. B. 1982. Timber loss estimates for the coniferous forests of the U.S. due to dwarf mistletoe. MAG Rep. 83-2. Fort Collins, CO: U.S. Department of Agriculture, Forest Service, Methods Application Group. 24 p.

Edminster, C. B.; Mowrer, H. T.; Mathiasen, R. L.; Schuler, T. M.; Olsen, W. K.; Hawksworth, F.G. 1991. GENGYM: A variable density stand table projection system calibrated for mixed conifer and ponderosa pine stands in the southwest. Res. Pap. RM-297. Fort Collins, CO: U.S. Department of Agriculture, Forest Service, Rocky Mountain Forest and Range Experiment Station. 32 p.

Hawksworth, F. G. 1959. Ballistics of dwarf mistletoe seeds. Science 130:504.

Hawksworth, F. G. 1961. Dwarfmistletoe of ponderosa pine in the Southwest. Tech. Bull. 1246. Fort Collins, CO: U.S. Department of Agriculture, Forest Service, Rocky Mountain Forest and Range Experiment Station. 112 p.

Hawksworth, F. G. 1977. The 6-class dwarf mistletoe rating system. Gen. Tech. Rep. RM-48. Fort Collins, CO: U.S. Department of Agriculture, Forest Service, Rocky Mountain Forest and Range Experiment Station. 7 p.

Hawksworth, F. G.; Johnson, D. 1989. Biology and management of dwarf mistletoe in lodgepole pine in the Rocky Mountains. Gen. Tech. Rep. RM-169. Fort Collins, CO: U.S. Department of Agriculture, Forest Service, Rocky Mountain Forest and Range Experiment Station. 38 p.

Hawksworth, F. G.; Johnson, D. W.; Geils, B. W. 1987. Sanitation thinning in young, dwarf mistletoe-infested lodgepole pine stands. Gen. Tech. Rep. RM-149. Fort Collins, CO: U.S. Department of Agriculture, Forest Service, Rocky Mountain Forest and Range Experiment Station, 2 p.

Hawksworth, F. G.; Scharpf, R. F. 1984. Biology of dwarf mistletoes: Proceedings of the symposium. Gen. Tech. Rep. RM-111. Fort Collins, CO: U.S. Department of Agriculture, Forest Service, Rocky Mountain Forest and Range Experiment Station. 131 p.

Hawksworth, F. G.; Wiens, D. 1996. Dwarf mistletoes: Biology, Pathology, and Systematics. Agriculture Handbook 709. Washington DC: U.S. Department of Agriculture, Forest Service. 410 p.

Hawksworth, F. G.; Williams-Cipriani, J. C.; Eav, B. B.; Geils, B. W.; Johnson, R. R.; Marsden, M. A.; Beatty, J. S.; Shubert, G. D.; Robinson, D. C. E. 1995. Dwarf mistletoe impact modelling system: User's guide and reference manual. Report MAG-95-2. Fort Collins, CO: U.S. Department of Agriculture, Forest Service, Methods Application Group. 120 p.

Hinds, T. E.; Hawksworth, F. G. 1965. Seed dispersal velocity in four dwarfmistletoes. Science 148: 517-519.

Moeur, M. 1985. COVER: a user's guide to the CANOPY and COVER extension of the Stand Prognosis Model. Gen. Tech. Rep. INT-190. Ogden, UT: U.S. Department of Agriculture, Forest Service, Intermountain Research Station. 49 p.

Myers, C. A.; Hawksworth, F. G.; Stewart, J. L. 1971. Simulating yields of managed, dwarf mistletoe-infested lodgepole pine stands. Res. Pap. RM-72. Fort Collins, CO: U.S. Department of Agriculture, Forest Service, Rocky Mountain Forest and Range Experiment Station. 15 p.

Robinson, D. C. E.; Geils, B. W. 2002. A spatial statistical model for the spread and intensification of dwarf mistletoe. Manuscript in preparation for Ecological Modelling.

Robinson, D. C. E.; Sutherland, G. D.; Bunnell, P.; Fairweather, M. L.; Shubert, G. D.; Taylor, J. E.; Geils, B. W. 1994 The new dwarf mistletoe spread and intensification model: final model review workshop report. Prepared by ESSA Technologies Ltd., Vancouver, B.C., for Methods Application Group, U.S. Department of Agriculture, Forest Service, Fort Collins, CO. 26 p. + appendices.

Robinson, D. C. E.; Sutherland, G. D.; Kurz, W. A. 2000. Simulating the effects of dwarf mistletoe in coastal western hemlock stands. Prepared by ESSA Technologies Ltd., Vancouver, B.C., for B.C. Ministry of Forests, Victoria, B.C. 48 p.

Shaw, D. C., Freeman, E. A.; Mathiasen, R. L. 2000. Evaluating the accuracy of ground based hemlock dwarf mistletoe rating: a case study using the Wind River Canopy Crane. West. J. Appl. For. 15: 8-14.

Shaw, D. C.; Weiss, S. B. 2000. Canopy light and the distribution of hemlock dwarf mistletoe (*Arceuthobium tsugense* [Rosendahl] G.N. Jones subsp. *tsugense*) aerial shoots in an old-growth Douglas-fir/western hemlock forest. Northwest Science 74: 306–315.

Stage, A. R. 1973. Prognosis model for stand development. Res. Pap. INT-137. Ogden, UT: U.S. Department of Agriculture, Forest Service, Intermountain Forest and Range Experiment Station. 32 p.

Strand, M. A.; Roth, L. F. 1976. Simulation model for spread and intensification of western dwarf mistletoe in thinned stands of ponderosa pine saplings. Phytopathology 66: 888-895.

Van Sickle, G. A.; Wegwitz, E. 1978. Silvicultural control of dwarf mistletoe in young lodgepole pine stands in Alberta and British Columbia. Report BC-X-180. Canadian Forestry Service, Victoria, B.C. 11 p.

Wykoff, W. R.; Crookston, N. L.; Stage, A. R. 1982. User's guide to the stand Prognosis model. Gen. Tech. Rep. INT-133. Ogden, UT: U.S. Department of Agriculture, Forest Service, Intermountain Research Station. 112 p.

Session 5. FVS in Modeling Systems